Section 8

Development of and advances in ocean modelling and data assimilation, sea-ice modelling, wave modelling

Modelling of superimposed ice formation during the spring snow melt period

Bin Cheng[1], Timo Vihma[2], Roberta Pirazzini[1,3] and Mats A. Granskog[4,5]

[1]Finnish Institute of Marine Research, P. O. Box 33, 00931 Helsinki, Finland

[2]Finnish Meteorological Institute, P.O. Box 503, 00101 Helsinki, Finland

[3]Department of Physical Sciences, P. O. Box 64, 00014 University of Helsinki, Finland

[4]Arctic Centre, University of Lapland, P. O. Box 122, 96101 Rovaniemi, Finland

[5] Present address: Centre for Earth Obs. Science, Univ. Manitoba, Winnipeg, Manitoba, Canada R3T 2N2

1. Introduction

In the sea ice modelling community, it is customary that ice melt is calculated both at the ice surface and bottom, but in many models ice growth is only considered at the ice bottom. In the melting season, however, formation of superimposed ice can take place via refreezing of surface snowmelt or rain. In March-April, 2004, an ice station was set up on land-fast sea ice in the Gulf of Bothnia, Baltic Sea. During the four-week period, the entire snow layer, originally 0.15 ± 0.05 m thick, was transformed to 7 cm of superimposed ice, except for 2 cm of snow that sublimated. We use observations of the meteorological conditions and radiative fluxes at the ice station for forcing a thermodynamic snow/ice model, while we use observations of the snow and ice evolution for the model initial conditions and validation, the latter being the basic motivation of this work.

2. Model experiments and results

A one-dimensional high-resolution thermodynamic snow/ice model (Launiainen and Cheng, 1998; Cheng and others, 2003) was used in this study. The following processes are taken into account in the model: heat conduction, penetration of solar radiation in the snow and ice, surface and subsurface melting, percolation of melt water to the snow/ice interface, refreezing of the melt water to superimposed ice, flooding of seawater and its refreezing, and bottom growth/melt of ice. In order to reproduce the exponential decay of penetrating solar radiation in snow and ice, high vertical resolution in a Lagrangian grid mode with 10 layers in the snow and 20 layers in the ice is used. Two strategies were applied: (A) forcing the model with parameterized air-ice fluxes, and (B) prescribing the air-ice fluxes according to the observations. Comparing the results of (A) and (B) against observations tells us about the relative importance of errors related to model forcing and modeling of the processes inside snow and ice. In both strategies, we also studied the model sensitivity to the snow/ice surface albedo.

The model results with the surface albedo prescribed according to the observations are referred to as the reference run (A_{REF}). In the first sensitivity test, A_P, the albedo was parameterized according to Perovich (1996). In the second test, $A_{FB,}$ the albedo was calculated acoording to Flato and Brown (1996), hereafter FB. A comparison of the time series of the observed and modelled snow and superimposed ice thickness is shown in Figure 1.

We made a simulation B_{REF} with the surface temperature, albedo, and radiative fluxes prescribed according to the observations (Figure 2). The evolution of the snow thickness from day 90 onwards is now better reproduced than in A_{REF}, which suggests that the internal processes in the snow cover are reasonably well modelled. In a sensitivity study B_{FB} the surface temperature and surface fluxes were prescribed according to the observations, as in B_{REF}, except that surface albedo is parameterized according to FB. Although the surface temperature is prescribed in B_{FB}, the parameterized albedo

affects both surface and subsurface melting. The results are, however, almost equal to those of B_{REF} with the prescribed albedo (Figure 2) due to the lack of feedback between the surface temperature and albedo. The importance of the feedback is demonstrated by the large difference between the results of A_{FB} (dashed lines in Figure 1) and B_{FB} (dotted lines in Figure 2).

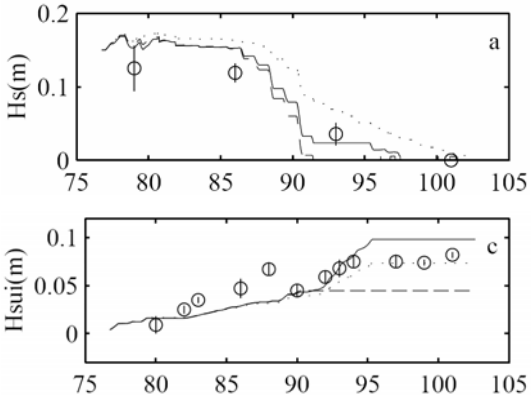

Figure 1. Observed and modelled evolution of (a) snow thickness H_s, and (b) superimposed ice thickness H_{sui}. The observations are marked by circles with the vertical bar indicating the spatial standard deviation. The solid lines indicate model results of A_{REF}, while the dotted and dashed lines indicate model results of A_P and A_{FB}, respectively.

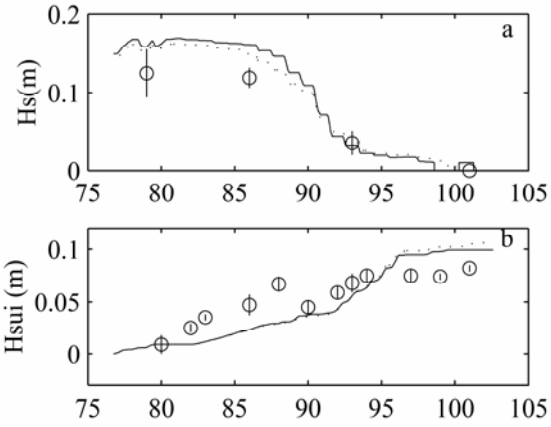

Figure 2. Observed (circles) and modelled evolution of (a) snow thickness and (b) superimposed ice thickness. The solid lines indicate results of B_{REF} while the dotted lines indicate results of B_{FB}.

3. Conclusion

A high vertical resolution was a needed for successful simulations. This is critical under conditions of large solar radiation and during rapid temperature changes. The modelled snowmelt and superimposed ice growth were consistent with the observations, but the net accumulation of superimposed ice was slightly overestimated. The modelled snow thickness was sensitive to the atmospheric forcing, and the influence was amplified when the albedo was parameterized as a function of surface temperature. In the sensitivity tests without this feedback, the direct effect of the inaccuracy in the albedo parameterization was minor. In further development of high-resolution thermodynamic snow and ice models, focus is needed on the parameterization of (1) surface albedo, (2) radiative fluxes, and (3) air-ice exchange during the night. In this study, surface temperature errors were not critical for the ice and snow mass balance, but in slightly warmer conditions equally large errors could have been critical if the erroneous simulations had not yielded freezing temperatures at night.

References

Cheng, B., T. Vihma and J. Launiainen. 2003. Modelling of the superimposed ice formation and sub-surface melting in the Baltic Sea. *Geophysica,* **39**(1-2), 31-50.

Flato, G.M. and R.D. Brown. 1996. Variability and climate sensitivity of landfast Arctic sea ice. *J. Geophys. Res.,* **101**(C11), 25,767-25,777.

Launiainen, J. and B. Cheng. 1998. Modelling of ice thermodynamics in natural water bodies. *Cold Reg. Sci. Technol.*, **27**(3), 153-178.

Perovich, D.K. 1996. The optical properties of sea ice. *CRREL Monogr*. 96-1.

Simulation of upper Ocean response to the observed cyclones in the Indian Seas

A.A.Deo, D.W.Ganer and P.S.Salvekar

Indian Institute of Tropical Meteorology, Pune 411 008, India
E-mail : aad@tropmet.ernet.in

Introduction

Ocean feedback factor (in particular upper ocean temperature) is important for dynamical prediction of tropical cyclones. In this study the oceanic response to the two cases of Indian Ocean cyclones (TC 01A) and (TC 02B) in 2004, is studied. The simple 1½ layer wind driven reduced gravity ocean model is employed for this study. The model derived Sea Surface Temperature change is validated with the observation for both the cases.

The first cyclone TC 01A (designated ARB0401 by IMD) formed early in the month of May just off the southwestern Indian coast. TC-01A (5 -10 May) moved erratically for several days, then began to move on a north- westerly trajectory paralleling the Indian coastline. Based on Joint Typhoon Warning Center's analysis, the system peaked at 23 m/s. The second cyclone TC 02B (designated BOB0401 by IMD), during the period 17-19 May, formed south of Kolkata, in Bay of Bengal and then moved east-northeastward, reaching hurricane intensity and smacking into the northwestern coast of Myanmar where it was quite destructive. The Indian Meteorological Department classified TC 02B as a Very Severe Cyclonic Storm implying winds in excess of 33 m/s.

Results and discussion

The reduced gravity model with horizontal resolution ½° x ½°, is integrated for the entire life span of these two tropical storms separately, from the initial condition of rest. The idealized cyclonic vortices suitable for these storms are used to force the model in separate numerical experiments. Figure 1 displays the results for the third day for the tropical storm TC 01A in the left panel and for TC 02B in the right panel. The first three figures in each panel are model derived currents, Mixed layer depth anomaly (MLDA) and temperature change for corresponding storm cases. The maximum currents of 0.6 m/s lie on the left of the track for TC 01A. Similarly, the MLDA and Temperature field also has left bias giving maximum upwelling (30 m) and maximum cooling (3 °C) on the left of the track. In the northern hemisphere tropical cyclones generally have maximum cooling in association with maximum upwelling to the right of the track [3,4] . The left bias may be due to the erratic nature of the storm track in the first three days. The storm travels southeastward for sometimes when there is looping of the track. Hence the bias is opposite to that of the earlier findings [1,2,3,4]. For the track of TC 02B the model currents, MLDA and temperature change, have right bias. The maximum currents of 0.2 m/s, maximum upwelling (7 m) and maximum cooling (3.5°C) are on the right of the track. The right bias is in agreement with the earlier model studies [1,2,3,4]. For both the tracks the surface circulation shows the divergence of the flow near the storm center. Also the region of upwelling (cooling) is surrounded by the region of downwelling (warming).

The model simulated temperature change is validated using observed temperature change from daily TMI SST, during the passage of the cyclones. This observed temperature change is shown in the last figure in each panel for both the tracks. It is seen that the observed cooling of 2.5 °C for TC 01A and 3.5 °C for TC 02B is well simulated by the models. The left bias in model temperature field for the cyclone TC 01 A and right bias for TC 02 B is also in agreement with the observed temperature change. The higher value of maximum cooling in the case of TC 02B as compared to TC 01A is attributed to the high intensity of the TC 02B over TC 01 A.

References

1. Chang S.W. & Anthes R.A., 1978: Numerical simulation of the ocean's nonlinear baroclinic response to translating hurricanes. J. Phys. Oceano., 13, 468-480
2. Price J.F., 1981: Upper ocean response to a hurricane. J. Phys. Oceano., 11,153-175.
3. Deo A. A., Ganer D.W. and Salvekar P.S., 2004: Behaviour of the upper ocean in response to an idealized symmetric and asymmetric Indian Ocean cyclone in opposite hemisphere., Jr. Ind. Geophys Uni, Vol. 8, no.3, pp 211-223

4. Deo A.A.., D.W Ganer. and P.S Salvekar, 2004: Numerical investigation of ocean mixed layer in response to moving cyclone : Sensitivity to model resolution', by, WGNE Report, Research activities in Atmospheric and Oceanic modelling, Report no. 34, pp 8.03 - 8.04

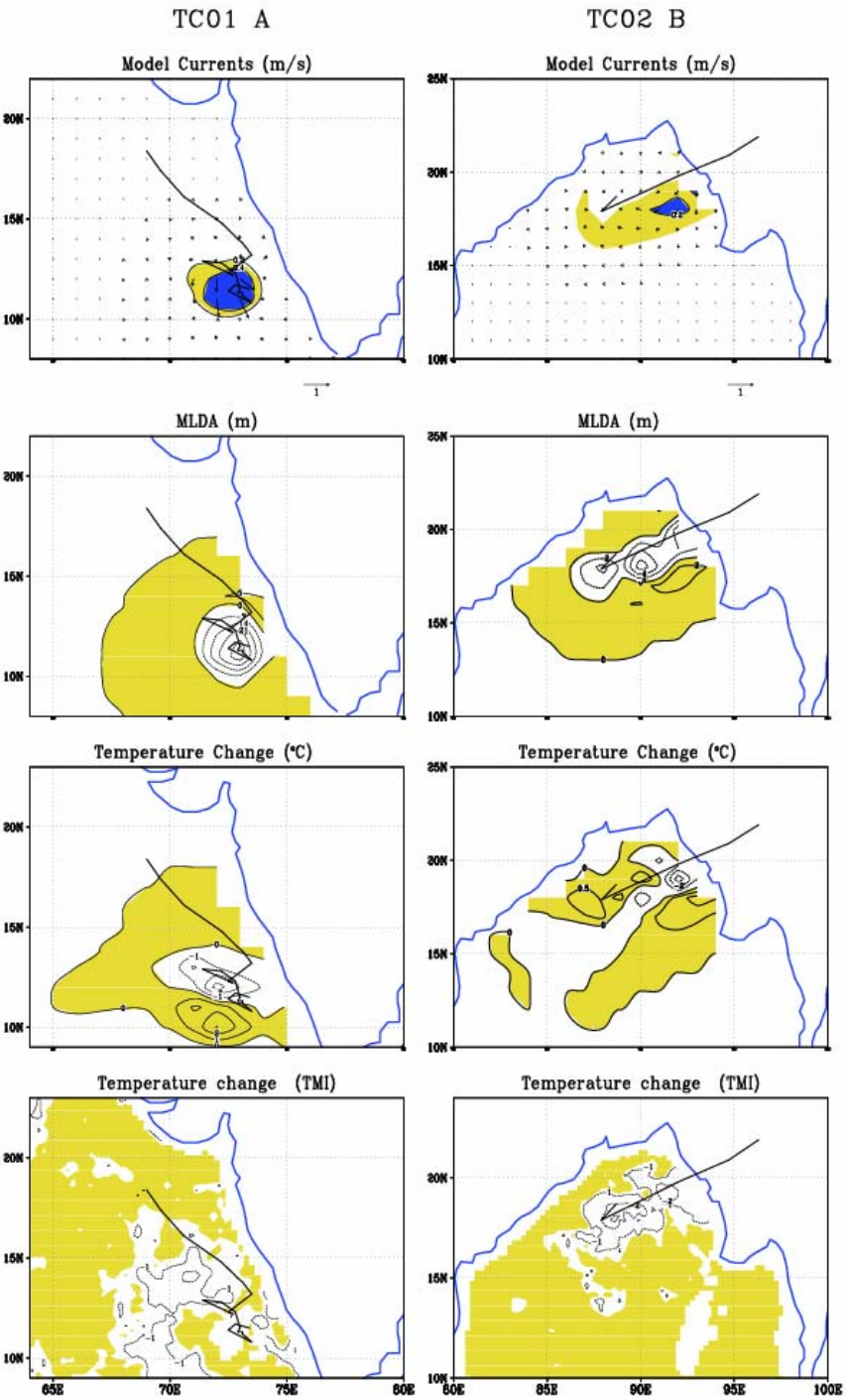

Model currents, Mixed Layer Depth Anomaly, Temperature change and observed temperature change on the third day for the two observed tracks (tracks shown as solid line). Positive values are shaded.

Baroclinic topographic waves on the Nicaragua Shelf generated by tropical cyclones

Dmitry S. Dukhovskoy, Steven L. Morey, and James J. O'Brien
Center for Ocean-Atmospheric Prediction Studies
Florida State University
Tallahassee, Florida, USA, 32306-2840
ddmitry@coaps.fsu.edu

1. Introduction

The present study is focused on the dynamic response of a stratified low-latitude ocean to tropical storms. In particular, cases of baroclinic coastally trapped waves generated by hurricanes passing over the Nicaragua Shelf are discussed. Tropical cyclones have a great impact on the ocean dynamics. Characterized by large wavelengths (O(10^3 km), strong wind-stress fluctuations, and long periods (weeks), these atmospheric systems influence the ocean dynamics on the scales from gravity waves to long waves which depend crucially upon the earth's rotation. The Caribbean Sea is strongly affected by tropical storms during the hurricane season. Since 1985 there were only two years (1992 and 1997) when the storms did not pass over the region.

2. Description of the region

In the Gulf of Mexico, hurricanes can generate barotropic shelf waves (e.g., *Morey et al.*, 2006). In the Caribbean Sea, due to very small Coriolis parameter (*f*), barotropic topographic shelf waves can be supported only over a very broad shelf due to large external Rossby radius of deformation ($R_e = f^{-1}\sqrt{gH}$, where *H* is the average depth). The shelf region near Honduras and Nicaragua, the Nicaragua Shelf, is the only wide shelf in the basin (~300 km in the widest place). However, the external Rossby radius for this location is ~ 700 km. Thus, barotoropic topographic waves can not be supported on this shelf. The presence of a sloping shelf break allows one to assume that internal topographic waves can exist in this region. The escarpment goes very shallow which permits one to suggest that atmospheric forcing can generate baroclinic waves along the shelf. Highly energetic positive wind stress curl imposed on the sea surface initiates isopycnal rise in the upper ocean through Ekman pumping. If the forcing moves towards the shelf break, the density anomaly follows it encroaching on the continental rise. This could produce strong baroclinic trapped motions. The typical slope of the shelf is ~10^{-2}. The range of stratification ($S = Nf^{-1}$) in the upper 50 m is ~200-300 which satisfies $\alpha > S^{-1}$. This allows trapped waves of type II, strongly trapped waves, following the classification of *Rhines* [1970].

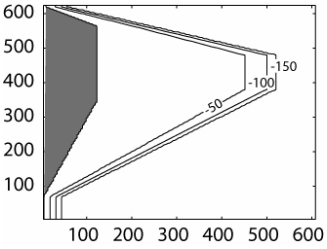

Figure 1. Model domain and bathymetry. Depth is in meters. The axes are distances (km).

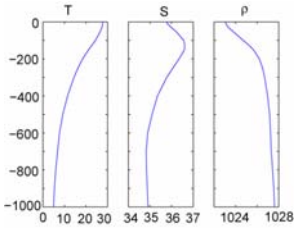

Figure 2. Temperature, salinity, and density profiles in the model.

3. Model experiment

To reproduce the mechanism described above, an idealized domain representative of the Nicaragua Shelf has been configured (Figure 1). The ocean is baroclinic and initialized with long-term average temperature and salinity profiles (Figure 2) (http://dss.ucar.edu). For simulation, the Navy Coastal Ocean Model (NCOM) is used with 10 σ-

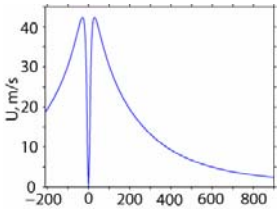

Figure 3. Wind speed profile in the hurricane used to force the model. The abscissa is distance from the hurricane center, km. The ordinate is

levels (Martin, 2000). The horizontal resolution is 4 km. The model is forced with a cyclonic wind stress from an analytical pressure wind field (Figure 3). The hurricane moves from the southeastern corner of the domain (lower right corner in Figure 1) to the northwestern corner (upper left) with a translation speed of 30 km h^{-1}.

The model results show (Figure 4) that when the density anomaly initiated by the moving hurricane hits the shelf break a baroclinic slope-trapped motion is produced. The wave phase moves with the shallow water to its right. Another type of wave is seen along the northern edge of the shelf (upper part of the domain). Since the coast in the model is approximated as a wall and not a sloping bottom, this is an interior Kevlin wave.

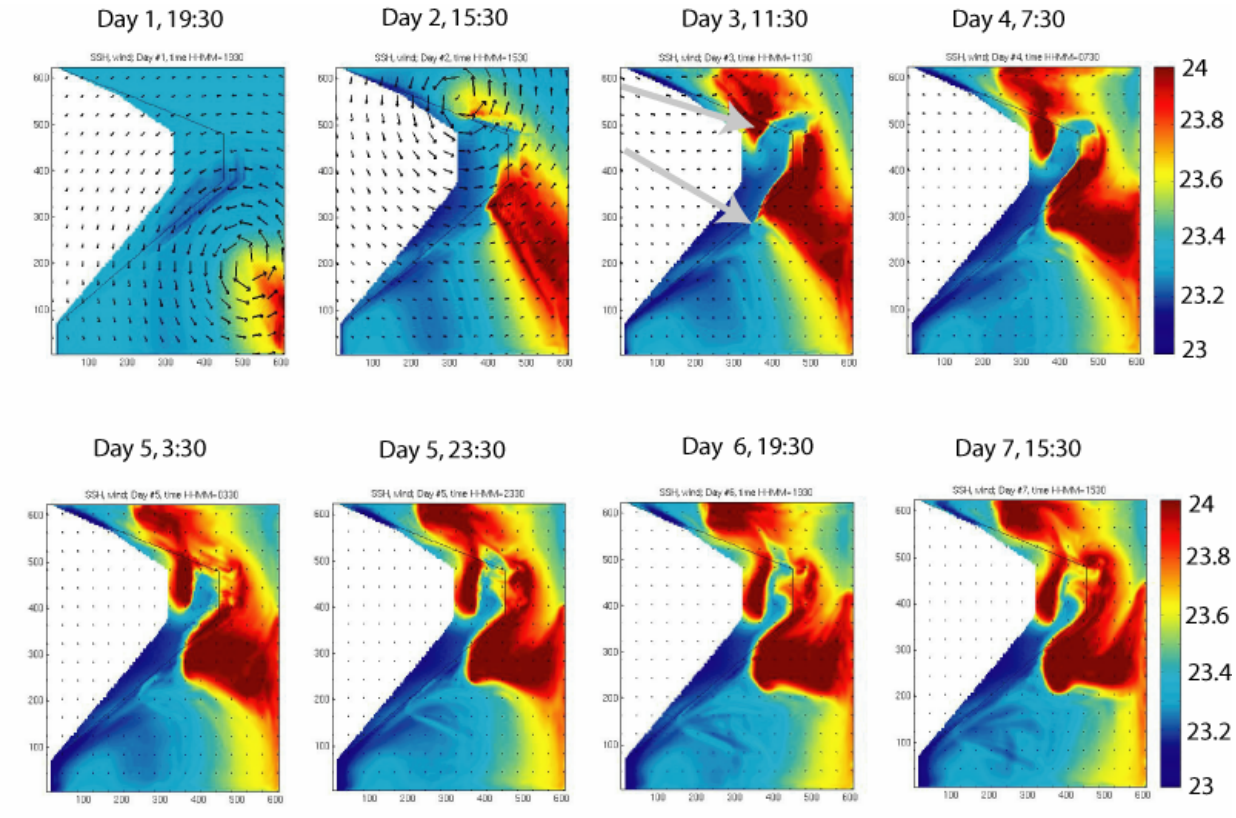

Figure 4. Simulated σ-density field at z = 30 m. Black arrows are wind vectors. Gray arrows in the panel "Day 3" indicate two baroclinic waves trapped along the topography. The upper wave is an interior Kelvin wave and the lower wave is a baroclinic topographic wave.

Acknowledgment

This project was sponsored by the Office of Naval Research Secretary of the Navy grant to James J. O'Brien, and by the NASA Office of Earth Science.

References

Morey, S.L., M. Bourassa, J.J. O'Brien, and D.S. Dukhovskoy, Modeling the impacts of remote forcing on hurricane storm surge, *Research Activities in Atmospheric and Ocean Modeling*, World Meteorological Organization, Submitted, 2006.

Martin, P.J., A description of the Navy Coastal Ocean Model Version 1.0. NRL Report: NRL/FR/7322-009962, pp. 39, Naval Research Laboratory, Stennis Space Center, MS, 2000.

Rhines, P.B., Edge-, bottom-, and Rossby waves in a rotating stratified fluid, *Geophys. Fluid. Dyn., 1*, 273-302, 1970.

Arabian Sea Warm Pool during two contrasting monsoons 2002 and 2003

[*]C. Gnanaseelan[1,2], Bijoy Thompson[1], J.S. Chowdary[1] , R. Deepa[1] and P.S. Salvekar[1]

[1] Indian Institute of Tropical Meteorology, Pune - 411 008
[2] Department of Meteorology, Florida State University, FL 32306
[* Email: seelan@tropmet.res.in]

Sea Surface Temperature (SST) over the South East Arabian Sea (SEAS) attains a maximum over 30^{o}C (warmest in the world ocean) during April - May, which is called as the Arabian Sea mini warm pool. The warming continues throughout the pre-monsoon period and it collapses with the onset of southwest monsoon. The warm pool location is very important in the sense that over this part of the Arabian Sea, the monsoon onset vortex (a depression which supports monsoon to its faster northward march) normally forms. One of the objectives of the Arabian Sea Monsoon Experiment (ARMEX) during 2002 and 2003 was to understand the mechanism responsible for the evolution and collapse of the Arabian Sea warm pool. The contrasting monsoon years (2002 and 2003) and the coincidental ARMEX observations during these years give a unique opportunity to understand how the ocean during this period responded to the local and remote forcing. The three-dimensional ocean model (POM) of the North Indian Ocean (NIO) [20^{o}S to 25^{o}N, 35^{o}E to 115^{o}E] is used to simulate temperature over the Arabian Sea warm pool region. The model forced by the accurate Quikscat winds could simulate the observed temperature and the temperature inversions in the southeast Arabian Sea region very well.

The early onset of Somali Jet in May, its disintegration in June and near disappearance in July have played major role in the drought-like situation over the subcontinent in 2002 monsoon. In contrast, stronger cross-equatorial flow during June-July 2003, has contributed substantially to the normal rainfall over the Indian subcontinent. Figure 1 compares the model simulated SST (the temperature of the first level) with the TMI SST for 2002 and 2003 respectively. The model SST's are well comparable with the TMI SST's over the entire Arabian Sea especially over the warm pool region. The model is able to reproduce the cooling of SST in July 2002 over Arabian Sea. Also in 2003 the model simulated SST shows a good agreement with TMI observed SST. The pre-monsoon warming and gradual decrease of SST over Arabian Sea with the advection of cold water from the Somalia coast were well represented by the model. Even though the 2002 monsoon was weaker, the cooling in the Somali coast during 2002 was found stronger than the 2003 season. Strong temperature inversions of about 1.5^{o} C magnitudes were recently observed in the XBT observations over the southeastern Arabian Sea and the adjacent regions at a depth of 20 to 40 m. The model could simulate these temperature inversions very well (Figure 2). The study found that the temperature inversions form every year and are mainly propagated from the Bay of Bengal. Also these inversions are found propagating westward along with the annual Rossby Waves (Figure not shown) in the Arabian Sea. The study also highlights the importance of accurate wind forcing in simulating the interannual variability in SST.

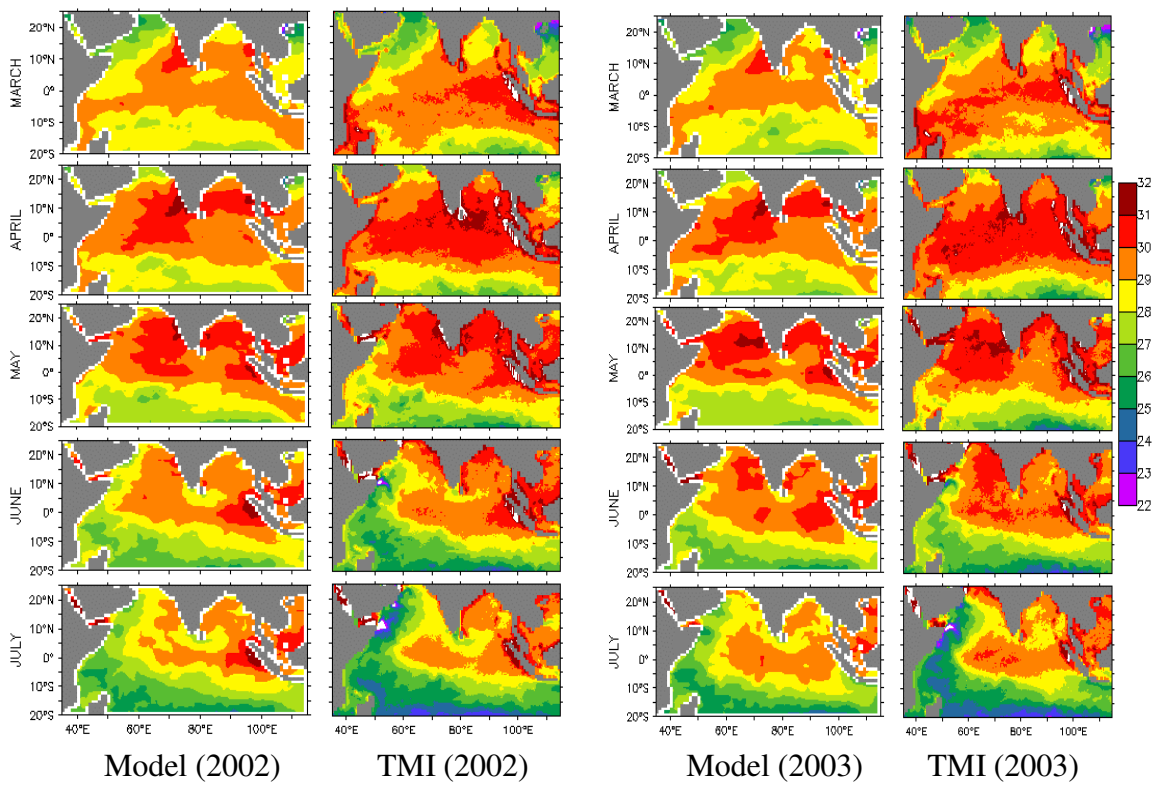

Figure 1: Observed and model simulated Sea Surface Temperature during 2002 and 2003

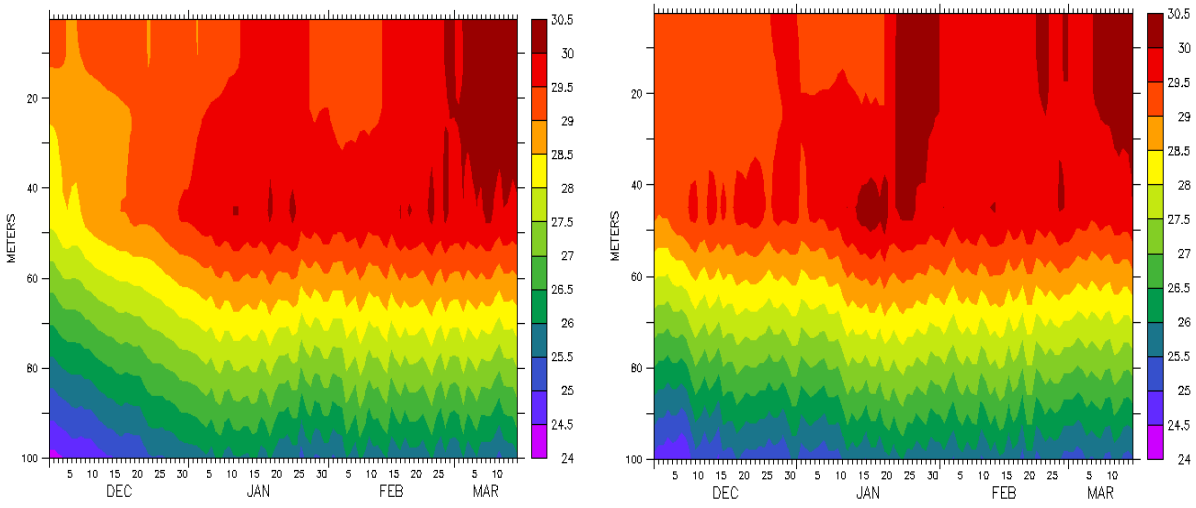

Figure 2: The Temperature inversions at 10 N, 75 E during December 2001 to March 2002 (left panel) & during December 2002 to March 2003 (right panel)

Modeling Tides on Semi-Enclosed Basin
A Case study of the Gulf of Mexico

Flavien Gouillon[1], Dmitry Dukhovskoy, Steven L. Morey and James J. O'Brien
Center for Ocean-Atmospheric Prediction Studies
The Florida State University

Tides are a well known process but a better understanding on how to implement them in a numerical model is needed. The main objective of this study is to seek the behavior of these tides in a semi-enclosed basin, in particular the Gulf of Mexico (GoM). The Navy Coastal Ocean Model (NCOM), a three-dimensional, hydrostatic, primitive equation model developed at the U.S. Naval Research Laboratory (Martin, 2000), is used to implement and seek the behavior of tides in the GoM. After a 30 day run to adjust the baroclinic model to initial fields, three experiments are conducted. The first one considers only the local tidal potential (LTP) on each node of the grid. This LTP is considered like an atmopheric pressure and is directly derived from the tidal equilibrium theory. The second method specifies barotropic transport and elevation of the tidal signal at open boundaries. The third one combines both previous methods of forcing tides. The t_tide Matlab© program (Pawlowiscz, 2002) is used to extract tidal constituents from surface elevation, with phase and signal-to-noise ratios. A spectral analysis is performed to see which frequencies are dominant in the Basin (Form ratio).

Results show that semi-diurnal tides in the GoM are dominantly forced by the local tidal potential whereas diurnal tides in the basin are driven at the boundaries. Combining both methods leads to a very realistic model of tides. In some specific areas, the surface elevation is amplified or de-amplified when the local tidal potential forcing is combined with the tidal signal propagating from the open boundaries. So the process of combining both methods is locally non linear. Ray tracing, by calculating the gradient of the phase in the basin, and integration of the local tidal potential along the rays (1) show some constructive and destructive interferences that can explain the tidal amplification and de-amplification. The impact of local tidal potential on altering the propagating tidal signal is calculated by integrating:

$$\frac{\partial \eta}{\partial t} = -K_{M2}(\omega_{M2} + \frac{2\pi}{T_{M2}})\cos^2\Phi \sin(\omega_{M2}\chi T_{M2} + \chi + 2\lambda) \qquad (1)$$

along the rays. Here, η is the surface elevation, K_{M2} general amplitude of M_2 constituent, ω_{M2} frequency of M_2 constituent, T_{M2} period of M_2, Φ is the latitude and λ is the longitude, χ is the phase of M_2 constituent at time t.

Figure 1 shows the surface elevation difference between the free propagating waves coming through the open boundaries and the LTP forced propagating waves on the

[1] Gouillon@coaps.fsu.edu

Florida West shelf. The Florida Big Bend ray is also shown. Integration along this path gives a difference of 0.017m and the net difference is 0.036m.

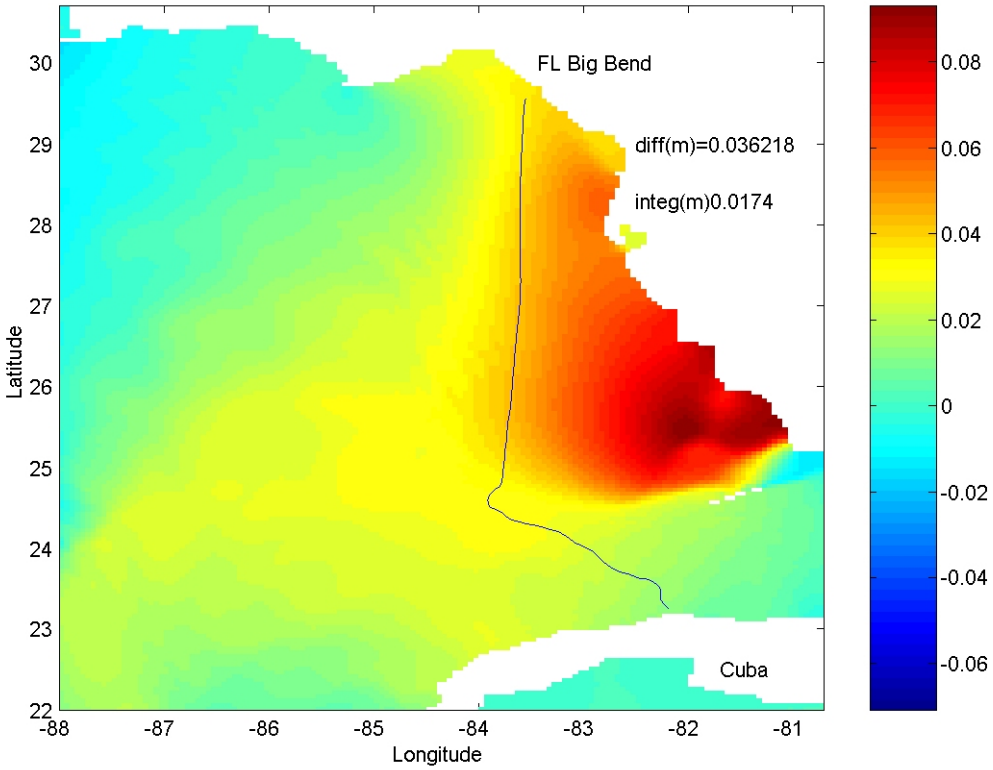

Figure 1: Surface elevation anomaly between free and LTP forced propagating wave (diff in meters) and ray tracing for the Florida Big Bend, integration of the LTP along the ray gives a constructive interference as the free propagating wave surface elevation is amplified by 0.0174 meter.

Numerical models of the GoM need to be accurately forced by the tidal signal at their open boundaries as it is the dominant forcing to get realistic tidal pattern. The LTP appears to be important in bays where the signal is easily amplified or de-amplified. It is clear that LTP is forcing the propagating waves in such a way that constructive interferences are possible in the West Florida Shelf. The work needs to be extended to the west part of the basin, particularly near the Bay of Campeche, where de-amplification is seen.

Acknowledgements

This research was funded by the Office of Naval Research through a Secretary of the Navy grant awarded to Dr. James J. O'Brien, and by a NASA Office of Earth Science grant.

References

Martin, P.J., A description of the Navy Coastal Ocean Model Version 1.0, NRL Report: NRL/FR/7322-009962, Naval Research Laboratory, Stennis Space Center, MS, 39 pp. 2000.

Pawlowiscz, R., B. Beardsley, and S. Lentz, 2002. Classical Tidal Harmonic Analysis Including Error Estimates in Matlab using T_Tide. *Computer and Geosciences*

Using Neural Network to Enhance Assimilating Sea Surface Height Data into an Ocean Model

Vladimir Krasnopolsky, Carlos J. Lozano, Deanna Spindler, Ilya Rivin, and D.B. Rao

***Abstract*—A generic approach that allows extracting functional nonlinear dependencies and mappings between atmospheric or ocean state variables in a relatively simple analytical form is presented. These dependencies and mappings between the 2- and 3-D fields of the prognostic and diagnostic variables are implicitly contained in the highly nonlinear coupled partial differential equations of an atmospheric or ocean dynamical model. They also are implicitly contained in the numerical model output. An approach based on using neural network techniques is developed to extract the inherent nonlinear relationship between the sea surface height anomaly and the other dependent variables of an ocean model. Specifically, numerically generated grid point fields from the Real Time Ocean Forecast System (RT-OFS) model of NCEP (National Centers for Environmental Prediction) are used for training and validating this relationship. The accuracy of the NN emulation is evaluated over the entire domain of the NCEP's RT-OFS. The differences in the accuracies of the technique in the coastal areas and in the deep water are discussed. Accurate determination of such relationships is an important first step to enhance the assimilation of the sea surface height measurements into an ocean model by propagating the signal to other dependent variables through the depth of the model.**

I. Introduction

The output of any complex geophysical numerical model, like models for numerical weather prediction, climate and ocean simulations, contains a great amount of data in the form of 2- and 3-D high resolution numerical fields of prognostic and diagnostic variables. This output contains, in an implicit form, the highly complex functional dependencies and mappings between the dependent state variables of the model. These relationships are governed by the physics and dynamics of the numerical model that has been used for the simulations. A clear understanding of the underlying nonlinear dependencies is a matter of great scientific interest and practical importance.

For example, when 2-D observations like surface wind, surface currents, or sea surface elevation are assimilated in the atmospheric or oceanic data assimilation system (DAS), the impact of this data in the DAS is localized at the level of their assimilation because there is usually no explicit mechanism in the DAS to propagate the impact of these data to other vertical levels and to other variables. Usually this propagation occurs later, during the time integration of the model, in accordance with dependencies determined by the model physics. Recently several attempts have been made to extract simplified linear dependencies of such a kind from observed data [1] or model simulations [2] for the use in an ocean DAS. However, these simplified and generalized linear dependencies that are often derived from local data sets do not properly represent the complicated nonlinear relationship between the model variables. If we were able to extract/emulate these dependencies in a simple, but not overly simplified, and yet adequately nonlinear analytical form, they could be used in the DAS to facilitate a more effective 3-D assimilation of the 2-D surface data. These analytical functions and mappings could also be used for efficient model output compression, archiving, and dissemination, and for sensitivity studies and error analysis.

Existence of a generic technique that would allow extracting these nonlinear functions and mappings in a compact analytical form would greatly facilitate the use of model output for qualitative and quantitative studies. Here we introduce a generic NN technique to accomplish this objective using a particular application (the NN emulation for sea surface height). This new and generic NN application requires a reasonable quality of the Jacobian of the NN emulation. The Jacobian analysis and an ensemble approach to improve the quality of the NN emulation and NN Jacobian are presented in [3].

II. SSH Mapping and its NN Emulation

A. Ocean Model

Sea surface height (SSH), η, is one of the prognostic variables in ocean circulation models. The particular ocean model that was used in this study is the HYbrid Coordinate Ocean Model (HYCOM). This model is a primitive equation model that uses a generalized hybrid coordinate (isopycnal/terrain following (σ)/z-level) in the vertical (see [4] for details). The hybrid coordinate extends the geographic range of applicability of traditional isopycnal coordinate (coordinates that follow the selected levels of constant water density) circulation models, toward shallow coastal seas and unstratified parts of the ocean. The particular version of HYCOM used in this study has a domain that covers the entire Atlantic Ocean with an average horizontal resolution of ⅓°; and 25 vertical levels.

V. Krasnopolsky, C. J. Lozano, D. Spindler, I. Rivin, and D.B. Rao are with the National Centers for Environmental Prediction, Camp Springs, MD 20746 USA (corresponding author V. Krasnopolsky phone: 301-763-8000 x 7262; fax: 301-763-8545; e-mail: Vladimir.Krasnopolsky@ noaa.gov).

B. Developing the Mapping

A suitable choice of input variables is required to discover the desired relationship from the model states. The reduced physics is the hydrostatic equation. Since the reduced physics model has mainly a 1-D vertical structure, we assumed, in this initial attempt, that SSH, or η, at a particular model grid point (i.e., at a particular horizontal location lat/lon) depends only on the vector of state variables X at the same horizontal location. Therefore, this dependence (a target mapping) can be written as

$$\eta = \phi(X) \tag{1}$$

where ϕ is a nonlinear continuous function and X is a vector that represents a complete set of state variables, which determines SSH. In this particular case the vector X was selected as $X = \{I, \theta, z_{mix}\}$, where I is the vector of interfaces (vertical coordinates used in HYCOM), θ is the vector of potential temperature, and z_{mix} is the depth of the ocean mixed layer (a total of 50 variables). This set of variables represents (or used as proxy for) the physics of the deep ocean. Therefore, the mapping (1) with this particular selection of components for the vector X will not be applicable in costal areas (depth less then 250 – 500 m). For the coastal areas a different set of state variables should be selected.

The NN technique is applied to derive an analytical NN emulation for the relationship between model state variables, X, and SSH, or η,

$$\eta_{NN} = \phi_{NN}(X) \tag{2}$$

using the simulated model fields which are treated as error free data. These fields are simulated by the model without data assimilation. A simulation that covers almost two years (from Julian day 303, 2002 to 291, 2004) was used to create training, validation and test data sets. Each data set consists of records $\{\eta_i, X_i\}_{i = 1,\ldots,N}$ collocated in space and time and uniformly distributed over the model domain.

C. Evaluating the Mapping Accuracy

The accuracy of the NN emulation is evaluated over the model domain (with coastal areas excluded). Several NNs were trained that have 50 inputs and one output in accordance with the dimensionalities of the target mapping (1). The NN emulation was applied to the last day of the entire simulation. This day is separated by the time interval of about eight month from the last day of simulation used for training and validation (52, 2004). Fields generated by the model at 00Z were used to create inputs, X, for the NN emulation (2). Then the NN emulation (2) was applied over the entire domain (with coastal areas excluded) to generate 2-D field of η_{NN}. This field was compared with the corresponding field of SSH, η, generated by the model. The difference between two fields is shown in Fig. 1. With the exception of several spots (most of them are still close to the coastal areas) the difference does not exceed ± 10 cm. The accuracy of the NN emulation over the entire domain shown in Fig. 1 is considered to be satisfactory: the bias is about 1cm and RMSE is about 4.7 cm. This conclusion that the accuracy of the NN emulation (2) is adequate is based on the fact that the NN emulation will be used in the DAS using satellite measurements of SSH that have an accuracy of order of 5 cm (or less).

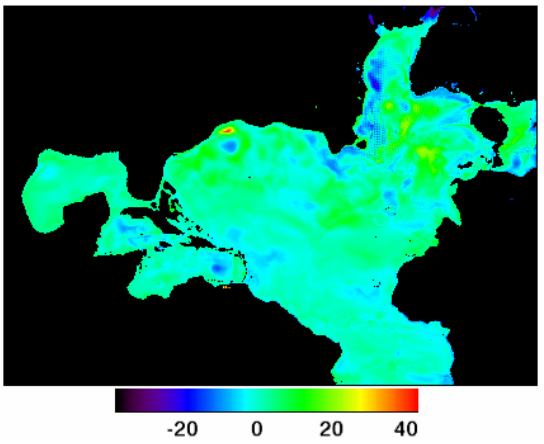

Fig.1 The difference (in cm) between SSH field and η_{NN} emulated by NN (2) with 5 hidden neurons.

III. Conclusion

In this paper we presented a generic NN approach that can be used to extract functional nonlinear dependencies and mappings between atmospheric and/or oceanic state variables using outputs from a numerical ocean model. These functions and mappings can be extracted in a closed, compact analytical form of NN emulations. Here we considered one particular application of this approach: using NN emulation of a mapping between a surface and subsurface parameters to enhance the data assimilation of a surface parameter (SSH) in the ocean DAS.

The availability of such NN emulations would greatly facilitate qualitative and quantitative studies of model output in general. These analytical functions and mappings could also be used for efficient model output compression, archiving, dissemination, and for sensitivity studies, and error analysis.

References

[1] S. Guinehut, P.Y. Le Traon, G. Larnicol, S. Philipps, "Combining Argo and remote-sensing data to estimate the ocean three-dimensional temperature fields – a first approach based on simulated data", *J Marine Systems*, 46, pp. 85-98, 2004

[2] G. L. Mellor and T. Ezer, "A Gulf Stream model and an altimetry assimilation scheme", *J Geophys. Res.*, 96, pp. 8779-8795, 1991

[3] V. M. Krasnopolsky, "Calculation of a stable NN Jacobian using an ensemble approach", *Proceedings of the IJCNN2006, July 16-21, 2006*, Vancouver, BC, Canada, 2006, in press

[4] R. Bleck, "An oceanic general circulation model framed in hybrid isopycnic-cartesian coordinates", *Ocean Modell.,* 4**,** pp. 55–88, 2002.

Operational Implementation of a HYCOM Based Real Time Ocean Forecast System (RTOFS) for the Atlantic Ocean Basin.

Carlos Lozano, Avichal Mehra, Chandra Narayanan, Desiraju B. Rao, Ilya Rivin
Marine Modeling and Analysis Branch/EMC/NCEP/NOAA,
Washington, D.C., USA

A Real Time Ocean Forecast System (RTOFS) for the Atlantic Ocean Basis has been tested and implemented into the operational suite of NCEP in December 2005. The dynamical engine of the RTOFS is the HYbrid Coordinate Ocean Model (HYCOM). For the Atlantic system HYCOM is configured for higher resolution in the western and northern portions of the basin and on shelves (3-7 km), in order to provide higher resolution alongthe U.S. coast rather than toward the east and southeast (7-13km). The model domain is an Atlantic Sector, from 20S to 76N including marginal seas, except for the Mediterranean and Baltic Seas. This system (see the web page http://polar.ncep.noaa.gov) provides a nowcast and a five day forecast once every day. The atmospheric momentum, heat and water fluxes are derived from three hourly NCEP GDAS fields. River outflows are derived from observations in the US coasts and climatology derived from RIVDIS elsewhere.

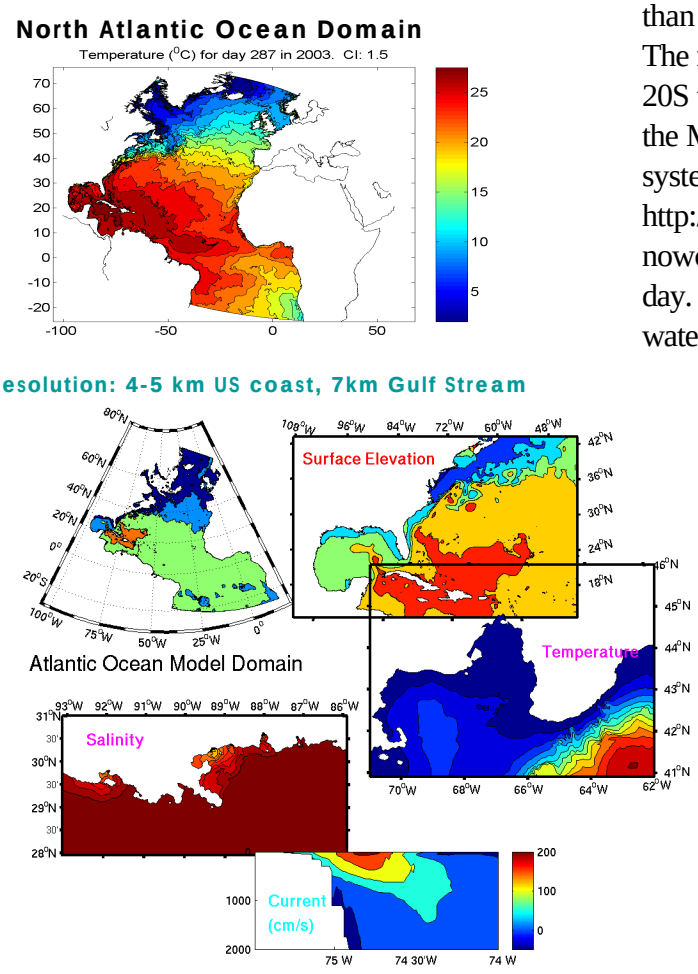

The figures to the left show the domain of the Atlantic Basin with SST and some surface ocean variables in selected sectors of the domain as examples.

Tidal forcing from body and boundary forcing is included in the model. The boundary tide data is taken from OSU TPX06 model. A comparison with the semi-diurnal tidal constituent M2 in the domain is shown in the figure below.

TIDES and OPEN BOUNDARIES in HYCOM

Boundary-tide: 1 invariant, AND body tide

TPX

Only body tide

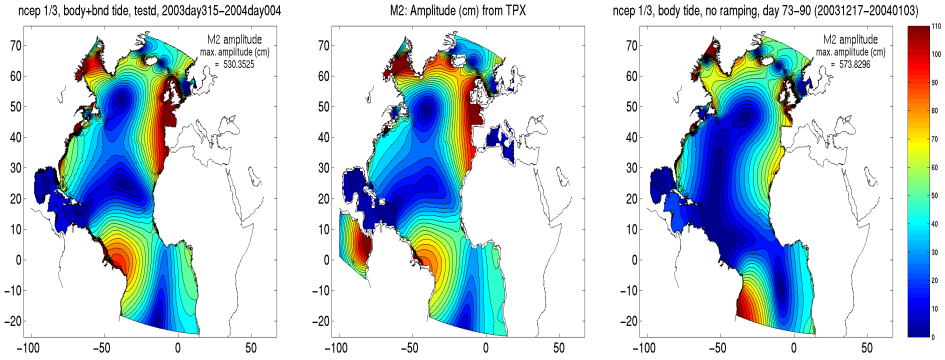

In the operational version, the model includes assimilation of remotely sensed and in-situ sea surface temperature. Assimilation of remotely sensed seas surface height anomalies and subsurface data will be introduced shortly.

The goals of the NOAA system are a) to provide accurate estimates in the coastal oceans for various applications such as containment of toxic spills, search and rescue missions, ecosystem monitoring and modeling, etc.; b) form part of the backbone for NOAA's and other institutions' regional ocean models by providing initial and boundary conditions; c) coupled circulation-wave-storm-surge models; and e) coupled atmosphere-ocean hurricane forecasts.

The Black Sea Nowcasting and Forecasting System Development

Petr N. Mikheev

Hydrometeorological Research Center of the Russian Federation,
Bol. Predtechesky per., 11-13, 123242 Moscow, Russia
E-mail: pmikheev@gmail.com

The Black Sea is a unique nearly landlocked sea basin characterized by strong density stratification. As a result of it, the permanent deep-water anoxic layer occupies 87% of the Black Sea volume. Human-induced changes in the Black Sea environment create an acute need for a research and development program designed to study different aspects of nonequilibrium ecosystems of the sea through a wide cooperation of the Black Sea countries in the field of observations, modeling, and analysis of sea variables.

The European Union funded project "A Regional Capacity Building and Networking Programmer to Upgrade Monitoring and Forecasting Activity in the Black Sea Basin" (ARENA) is one of such cooperative programs aiming at regional capacity building in close collaboration with regional and other relevant organizations. In the context of this project at the Hydrometcenter of Russia, Princeton Ocean Model (Mellor, 2003) and its version ECOMSED (Blumberg, 1996) are used for the extensive calculations of the Black Sea water circulation, temperature and salinity. Princeton Ocean Model (POM) is a sigma coordinate, free surface, primitive equation ocean model, which includes a turbulence sub-model developed in the late 1970's by Blumberg and Mellor, with subsequent contributions from other people (Mellor and Yamada, 1982). POM uses an orthogonal curvilinear coordinate system, which greatly increases model efficiency in treating irregularly shaped coastlines and in meeting requirements for high resolution at desired locations. The model has been successfully used in modeling estuaries, coastal regions, and open oceans. The latest version of POM is the ECOMSED model including three main sub-models. These are hydrodynamic module, sediment transport module, and wind induced wave module. The sediment transport module is of great importance in modeling water ecosystems.

Research in 2005 was focused on the adaptation of the models (POM and ECOMSED) to the Black Sea, upgrading of the computational model grids to high resolution, and near-real time data assimilation. The entire system can be separated into four main components: (1) the model's module; (2) the generation of the computational grids; (3) the generation of the temperature and salinity fields (initial conditions); (4) the atmospheric forcing (boundary conditions).

Fine grids are required for the Black Sea hydrodynamic model applications even if the computational time may greatly increase. The generation of the computational grids using the computer graphics methods is an example of such module (Mikheev, 2005). Grid cells are determined by the boundaries and by the number of grid junctions along each latitude and longitude. The land-sea mask taking into account the irregularly shaped coastline is produced by the Weiler and Atherton algorithm (Weiler and Atherton, 1977). Then the 2-Minute Gridded Global Relief Data (ETOPO2, Boulder World Data Center for Marine Geology & Geophysics) are interpolated into this grid. The longitudinal and latitudinal resolution varies between 6 and 14 km, thus, better describing the Black Sea coastline. The maximum model depth is 2200 m and there are 31 vertical sigma levels.

The module of the generation of initial conditions uses the MEDAR/MEDATLAS temperature and salinity annual and monthly distributions interpolated at 25 horizontal levels and objectively analyzed to produce grided climatological fields. The goal of the MEDAR/MEDATLAS II project is to rescue, safeguard, and make available a comprehensive data set of oceanographic parameters collected in the Mediterranean and Black Sea through a wide cooperation of the Mediterranean and Black Sea countries. The atmospheric forcing is based on the analyses received daily from the Global medium-range weather forecast model developed in the Hydrometcenter of Russia or from the National Center for Environmental Prediction (NCEP), Washington.

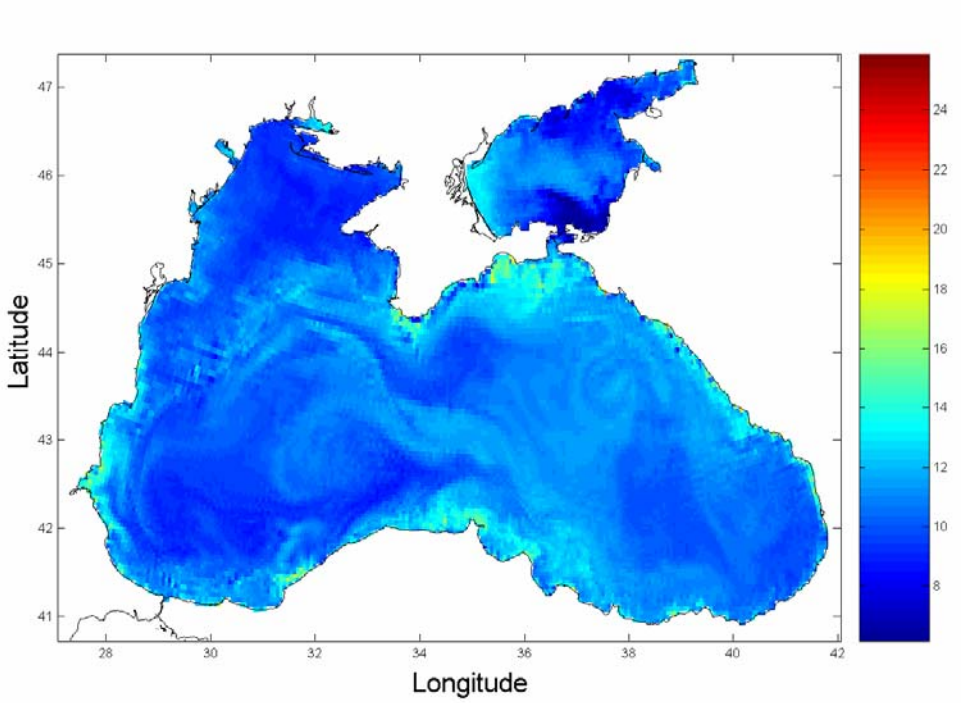

Figure 1. An example of model results: sea surface temperature distribution for February.

The model capacity to represent specific Black Sea physical properties (cyclonic Rim current, presence of the permanent cold intermediate layer in the temperature field, seasonal intensification of the cyclonic circulation) is shown by the comparison of model results with satellite and observational data and with published results from other models for the Black Sea area with similar configuration. Figure 1 shows the February temperature distribution obtained with our configuration of POM.

It is planned to advance this system in the nearest future. Until present, the interconnected Black Sea - Mediterranean Sea basin systems has been poorly addressed in numerical model studies. The exchange flows between the seas are not well studied yet. Many questions exist about the impact of the Kerch and Bosphor Straits on physical characteristics of the Black Sea. There are great uncertainties in values of the horizontal and vertical eddy viscosity and vertical diffusivity coefficients. We are going to investigate these questions in our further studies. It is planned to compare the modeling results with the altimeter data in order to improve the monitoring of the Black sea circulation. This prototype of the Black Sea nowcasting and forecasting system is regarded as a first stage to further develop the Black Sea operational marine forecasting and research system at the Hydrometcenter of Russia.

References

Mellor, G. L., Users guide for a three-dimensional, primitive equation, numerical ocean model (June 2003 version), 53 pp., Prog. in Atmos. and Ocean. Sci, Princeton University, 2003.

Blumberg, Alan F., (1996). “An Estuarine and Coastal Ocean Version of POM”. Proceedings of the Princeton Ocean Model Users Meeting (POM96), Princeton, NJ.

Mellor, G.L. and T. Yamada, "Development of a Turbulence Closure Model for Geophysical Fluid Problems," Rev. Geophys. Space Phys., 20, 851-875, 1982.

Weiler, K. and P. Atherton, "Hidden Surface Removal Using Polygon Area Sorting," ACM Computer Graphics (SIGGRAPH `77 Proceedings), vol. 4, no. 3, pp. 214-222, July 1977.

Mikheev, P.N., "Using Methods of Computer Graphics for the Generation of Ocean Model Numerical Grids," Proceedings of Mathematical Methods of Image Data Recognition Meeting (2005), Moscow, Russia.

Sutherland I.E., Hodgman G.W. Reentrant Polygon Clipping // Communications of the ACM, 17(1), pp. 32-42, 1974.

Mixed Layer dynamics and thermodynamics in the Central Arabian Sea

A.K. Mishra[1,2] and C. Gnanaseelan[1,2]
[1] Indian Institute of Tropical Meteorology, Pune – 411008, India
[2] Department of Meteorology, Florida State University, FL – 32306

In this study we highlight the importance of vertical advection in SST evolution in the central Arabian Sea. We used 1-D models to understand the different oceanic processes responsible for the temperature changes in this region. Data used in this study is the intensive buoy observations at 15.5° N, 61.5° E during October 15, 1994 to October 20, 1995, deployed off the coast of Oman to collect the near surface meteorological and oceanic data and to prepare the unique time series. It is important to mention that the point considered here is close to the Findlater jet (climatological maximum wind speed during the southwest monsoon). The monthly mean climatological SST at 15.5° N, 61.5° E is bimodal in nature with a primary maximum during May-June (i.e. around 29° C), and a secondary maximum in October (27.5° C). In response to the summer monsoon forcing during June to August, the sea surface cools by about 4° C.

For the complete understanding of the thermodynamics of the Arabian Sea we used the one dimensional dynamic instability model Price Weller Pinkel (PWP) and the Mellor- Yamada (turbulence-closure level 2.5 model) model (MY). These models have performed well for the Pacific and Atlantic oceans, they were recently used in the Indian Ocean also. One year long time-series of observed heat and momentum flux data were used to force these models. The models have performed reasonably well in simulating the SST except for the SW monsoon season (i.e. June to September). The SST simulated by the PWP model was about 5° C higher than the observed (Figure 1), which strongly emphasizes the role of advection and the vertical mixing in determining SST during SW monsoon season. Apart from the advection of cold water, the local entrainment and surface heat losses are also responsible for the drop in the SST. But the WHOI observations revealed that the net heat flux to the ocean was positive (of the order of 48 W/m^2 in June and 56 W/m2 in July) during the SW monsoon-95, which clearly indicates that the cooling is due to the local entrainment resulting to the mixed layer deepening and advection of cold water from the coast. We did a set of sensitivity experiments and found that vertical mixing is playing a key role in the SST evolution over this region. The increased mixing in PWP however helped to simulate SST very well (Figure 2).

To understand the transport of mass and heat at different levels, the current and temperature profiles up to 100 m are analyzed in detail. In top 50 m, the current was close to 5 cm/s. During April surface currents were eastward, whereas at 10 m, the transport was from west-southwest. It was from west to east from 20 m to 50 m, below that the relatively stronger current at 65 m was observed (west north west). During April, SST was around 28.5° C and the mixed layer depth (MLD) was approximately 18 m. Strong south south-westerly (SSW) winds (10 m/s) was observed in June. The current speed in top 40 m also increased in June. Due to the strong winds, the Ekman current (drift) (i.e. current direction is 45° right from the wind direction in NH) was observed. It is a clear indication that the currents are dominated by Ekman drift. In the top 40 m the current decreases with depth but had constant eastward direction (from the Oman coast). During July, the mean monthly southwesterly winds of speed 12.37 m/s were observed. Average

current at each level was 2.5 times of June currents. Strong wind supported the Ekman drift, which resulted the surface current of about 40 cm/s flowing eastward. During July, the direction of the current in the top 100 m was almost constant (eastward). Coastal upwelling along the coast of Oman and upwelling in the Socotra eddy region and its possible advection may be contributing in the July cooling. High wind speed during July supported the entrainment cooling and deepening of the mixed layer. Strong currents in the upper layer bring the cold water towards the point of observation, which result in the mixed layer cooling. MLD was 65-70 m during July and the SST was about 27° C, which is about 1° C less than the June SST. Wind speed decreased to about 9.33 m/s in August, and there was no Ekman drift in the surface current. Current profiles of August revealed that the strongest surface currents of 55 cm/s were observed at the surface coming from the Oman coast. The current speed decreased with depth, but at all the levels they were the seasonal maxima. August SST was 26° C, i.e. 1° C less than that of July, whereas the mixed layer shoaled (approximately 32 m). The August current direction was favorable to the advection of cold water from the coast of Oman. During September with the retreat of the monsoon winds were decreased to a low value of 6.82 m/s, currents also decreased to around 20 cm/s at the surface. MLD was 40 m, deeper than August and SST was above 27° C. The study revealed that the wind speed is controlling the mixed layer, both on diurnal scale and on monthly scale. The wind directions are also important in determining the mixed layer depth. In most of the cases the frequent changes in wind direction was responsible for the increase in MLD (diurnal scale). It is understood that the advection may be playing the important role in determining the SST in the Central Arabian Sea. So a dedicated three - dimensional model is essential to understand the internal dynamics in the Arabian Sea, especially during the monsoon season.

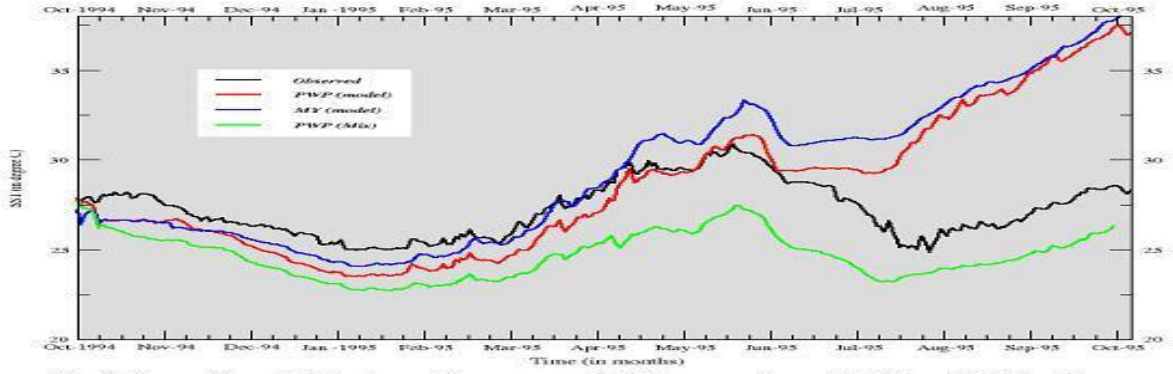

Fig. 1 Time series of SST observation compared with two versions of PWP and MY Model runs

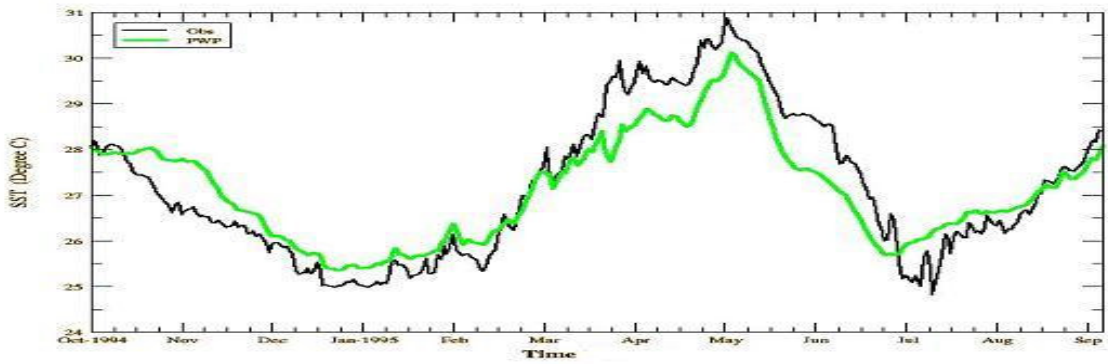

Fig. 2 PWP with increased mixing compared against observed SST

Modeling the Impacts of Remote Forcing on Hurricane Storm Surge

Steven L. Morey, Mark A. Bourassa, Dmitry S. Dukhovskoy, and James J. O'Brien

Center for Ocean – Atmospheric Prediction Studies
Florida State University
Tallahassee, FL 32306-2840
morey@coaps.fsu.edu

1. Introduction

On July 10, 2005, Hurricane Dennis made landfall just eastward of Pensacola, FL. About 275 km to the east, St. Marks, FL, and neighboring coastal communities of Apalachee Bay experienced a devastating storm surge estimated at 2.5 to 3 m, with even greater sea level maxima at some specific locations, making this the highest storm surge for the area since the 1920's. The surge caused extensive damage to private properties and local infrastructure, effectively isolating several communities. Official forecasts issued through public advisories from the National Hurricane Center (NHC) warned of a storm surge potential of only 4 to 6 feet (approximately 1.5 to 2 m) for this area. The extreme sea level rise is not obviously explained by the relatively weak (borderline tropical storm strength) winds measured along the coast and over the bay. This naturally leads to the question of the source of the additional 1 meter sea level rise in Apalachee Bay.

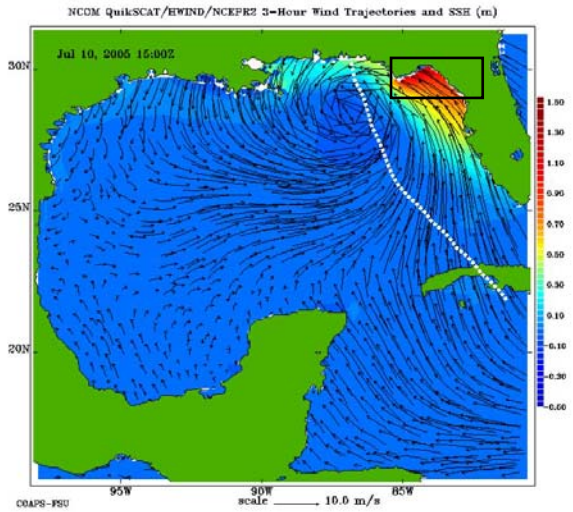

Figure 1. Modeled sea level anomaly with wind trajectories and schematic track of Hurricane Dennis overlaid with the dotted white line. The black box denotes the northeastern Gulf of Mexico nested model domain.

Storm surge models used to provide guidance for these official forecasts have a limited geographic domain, and thus do not include the effects of remotely generated sea level signals. Hurricane Dennis tracked northward, parallel to the West Florida Shelf (Figure 1), for several days. The hypothesis is that northward winds along the shelf generated a high sea level anomaly along the western coast of Florida, which then propagated northward as a topographically trapped wave. The wave was amplified by forcing from the storm, which traveled in the same direction as the shelf wave. This remotely generated wave could have increased the sea level in the northeastern Gulf (Apalachee Bay) by as much as one meter, adding to the local storm surge. This hypothesis is tested by running a series of experiments using nested models. The modeled wave nearly accounts for the excess sea level rise above the forecasts for this storm. The results from this exercise demonstrate the need for revising the modeling system currently used for predicting storm surge to account for remote influences, which can be important for storms the track parallel to coastlines.

2. The Experiments

The Navy Coastal Ocean Model [*Martin*, 2000] is configured for the Gulf of Mexico (GoM) domain (Figure 1) at 1/60° horizontal resolution and run in barotropic mode. A northeastern GoM subdomain is also defined (black box in Figure 1). Radiation open boundary conditions are applied along boundaries not on land. Wind fields are constructed by blending the NOAA AOML Hurricane Research Division H*Wind data [*Powell et al.* 1998] with NCEP Reanalysis II winds using the objective method described in *Morey et al.* [2005], where the H*Wind data are treated as "observations" in the objective method. The objectively gridded wind fields are computed at 1/8° resolution at time steps corresponding to the H*Wind fields (either every 3 or 6 hours) before interpolation to the model domain and model time step. Wind stresses are calculated using a quadratic drag coefficient formulation [*Morey et al.*, 2005].

The GoM barotropic model is integrated from rest applying the wind fields from July 8, 2005 0:00UTC to July 11, 2005 0:00UTC. Two additional experiments are conducted using the northeastern GoM domain. First, the limited-area model is integrated from rest with wind forcing. The radiation boundary condition is used along the western and

southern open boundaries. Second, this northeastern GoM domain is nested within the GoM domain, so that open boundary conditions are obtained from the large scale model. No local wind forcing is applied to the northeastern GoM model in this case. These experiments are designed to isolate the impacts of local forcing (in the first case) and remote forcing (in the latter case).

3. Results and Conclusions

The GoM model produces a storm surge maximum in Apalachee Bay as was observed during the storm (Figures 2 and 3). The locally forced sea level response in the northeastern GoM model is very small compared to the sea level rise modeled in the full GoM simulation. In the experiment with the northeastern GoM model forced only at the boundaries by nesting within the GoM simulation, a maximum sea level anomaly on the order of 1m is found in the northern Apalachee Bay.

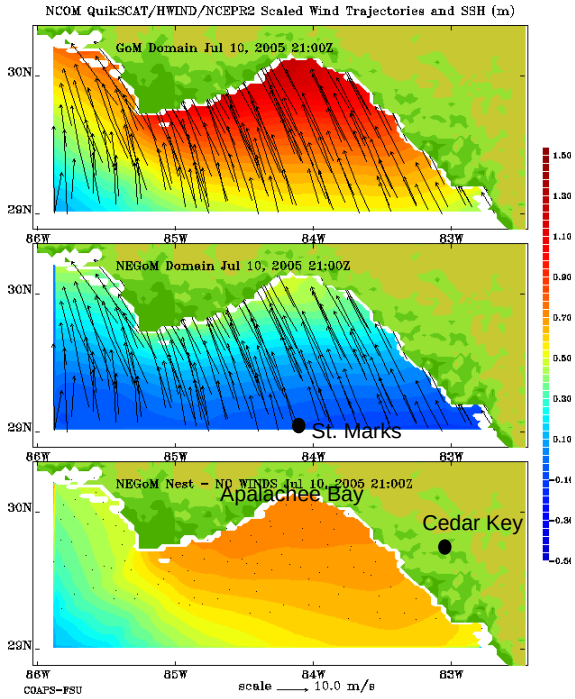

Figure 2. Modeled sea level anomaly with wind trajectories in Apalachee Bay for the northeastern region of the GoM model (top), the northeastern GoM model with local forcing (middle), and the northeastern GoM model with no local forcing nested inside the GoM model (bottom). Note that the experiments did not include the effects of atmospheric pressure, tides, wave setup, and small scale local bathymetric and coastline variations.

The unforced nested northeastern GoM model demonstrates the impacts of the remotely generated sea level signal on the sea level rise in Apalachee Bay. The signal propagated northward as a shelf wave (topographic Rossby Wave), and was reinforced by eastward Ekman transport toward the coast under the along-shore winds at the eastern side of the storm. Idealized shelf experiments have been used to validate this physical mechanism. Analysis of the sea level model fields shows that the sea level responds as a linear combination of the remotely generated sea level and the locally forced sea level (Figure 3).

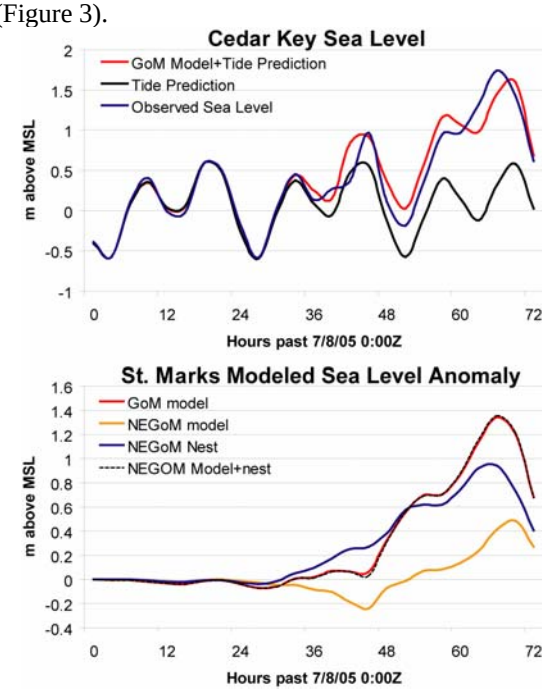

Figure 3. (Top) Modeled sea level anomaly plus tidal predictions plotted against observations at Cedar Key. (Bottom) Model sea level anomaly at St. Marks from the nested northeastern GoM model, locally forced northeastern GoM model, and the full GoM domain. The time series of the two northeastern GoM modeled sea level anomalies are added together and nearly match the full domain solution, demonstrating linearity of the sea level response to local and remote forcing.

Acknowledgements

This project was sponsored by NOAA as part of the Applied Research Center funding to COAPS. Thanks to Paul Martin and Alan Wallcraft at NRL for the NCOM development and their assistance with the model.

References

Martin, P.J., 2000: "A description of the Navy Coastal Ocean Model Version 1.0". NRL Report: NRL/FR/7322-009962, Naval Res. Lab., Stennis Space Ctr., MS, 39 pp.

Morey, S. L., M. A. Bourassa, X. J. Davis, J. J. O'Brien, and J. Zavala-Hidalgo (2005), Remotely sensed winds for episodic forcing of ocean models, *J. Geophys. Res.*, *110*(C10), C10024, doi: 10.1029/2004JC002338.

Powell, M.D., S.H. Houston, L.R. Amat, and N. Morisseau-Leroy (1998), The HRD real-time hurricane wind analysis system, *J. Wind Engineer. and Indust. Aerodyn.*, *77*, 53-64.

Transport of Waters from a Deep Convection Region in the Labrador Sea: Sensitivity of Trajectories to Initial Position and to Atmospheric Forcing

Yurii D. Resnyansky, Alexander A. Zelenko, and Boris S. Strukov

Hydrometeorological Research Center of Russian Federation,
Bol. Predtechesky per., 11-13, 123242 Moscow, Russia E-mail: resn@mecom.ru

The concept of water masses holds an important place in classical oceanography. The characteristic feature of water masses is their homogeneity, produced and sustained by turbulent mixing. The building-up of water masses, including the deep-sea ones, according to Zubov (1938), takes place somewhere at the water surface, mainly due to winter vertical circulation. And then they are transported, preserving the acquired properties, to different regions by large scale sea currents. In adhering to this concept it is implicitly assumed that the integrity of large volumes of water is ensured in the course of their transportation; that is to say, water particles close to each other at some time remain such also at any subsequent instant. There are certain reasons for the concept of this sort. First of all, these are fairly steady T-S-properties. That steadiness, in essence, is generally used to subdivide the bulk of ocean waters into individual water masses.

At the same time, in modern studies on geophysical hydrodynamics deterministic models of ocean processes with manifestations of chaotic behavior are proposed and are actively developed (e.g., Yang 1996). The origination of chaotic behavior in a broad class of that sort of models pertains to the presence of strong instability of trajectories relative to their original position. Given such instability, initially close water particles after a lapse of time may be found far apart.

At the present time analysis of trajectories, i.e. Lagrange description of motion, is intensively used in studies of spreading of contaminants and of other water properties in the ocean. Here we will take a look at the transport of fluid particles with a starting position in the Labrador Sea. The tracing of water transport from this region is of particular interest due to the fact that the Labrador Sea is one of a few regions, in which the waters transformed near the surface are then mixed down to great depths under the action of intensive density convection and, being picked up by large scale flows, fill out the abyssal area at first of the North Atlantic and then, through the global conveyor belt, of the whole World Ocean (Gordon 1986; Broecker 1991; Koshlyakov et al. 2001).

The time-dependent ocean currents appropriate for plotting the trajectories were determined from numerical experiments with an ocean general circulation model (OGCM) based on primitive equations (Resnyansky and Zelenko 1999) The computations were performed in the global domain (excepting the Arctic Basin to the north of 80.3° N) with a horizontal resolution $\Delta\lambda = 2°$, $\Delta\varphi = 2°$ ($\Delta\varphi \sim \cos\varphi$ to the north of 40° N) and 32 unevenly spaced levels in the vertical. The OGCM runs in numerical experiments started from rest with climatological January distributions of sea water temperature and salinity specified from data of the WOA-2001 atlas (Conkright et al. 2002). The NCEP–DOE AMIP-II reanalysis data on the surface heat, fresh water and momentum fluxes (Kanamitsu et al. 2002) were used as atmospheric forcing (AF) with 6-hour data point interval in experiment ***BASE*** and monthly smoothed data in experiment ***SMON***. The length of both integrations was 24 years (1979–2002 according to the calendar associated with data on AF). The output fields on sea currents were archived for subsequent plotting of trajectories with 5 days intervals.

Fig. 1 shows the trajectories of fluid particles emitted from 500 m depth at three relatively close points in the Labrador Sea. Not going into details of individual trajectories, only from a general view of the figure it may be concluded that initially close particles after a lapse of time are found in positions separated by thousands of kilometers in the lateral direction and by thousands of meters in depth. And all this occurs over relatively short for oceanic measures time intervals of 24 years. It is clear that in model integrations over hundreds and thousands years, which are characteristic times for building-up of thermohaline structure in deep ocean, the scatter should be still larger. Thus, the advective transport in the OGCM, used to generate data on ocean currents for trajectories plotting, possesses properties inherent in chaotic advection (e.g. Kozlov and Koshel 2000).

From the comparison of trajectories plotted from data in experiment ***BASE*** with 6-hourly AF and in experiment ***SMON*** with monthly smoothed AF (blue and red curves in the figure) it is also apparent that long distance transport essentially depends not only on initial positions, but also on short-term perturbations of current speed vector superimposed onto large scale seasonally varying circulation. This dependence is another manifestation of trajectories instability having as a consequence a phenomenon of the chaotic advection kind.

Acknowledgment: This work was supported by the Russian Foundation for Basic Research grant No. 06-05-64611.

REFERENCES

Broecker W.S., 1991: The great ocean conveyor. *Oceanography*, **4**, 79–89.

Conkright, M.E., R.A. Locarnini, H.E. Garcia et al., 2002: *World Ocean Atlas 2001: Objective Analyses, Data Statistics, and Figures, CD-ROM Documentation*. National Oceanographic Data Center, Silver Spring, MD, 17 pp.

Gordon, A.I., 1986: Interocean exchange of thermocline water. *J. Geophys. Res.*, **91**, 5037–5046.
Kanamitsu, M., W. Ebisuzaki, J. Woollen, S-K Yang, J.J. Hnilo, M. Fiorino, and G. L. Potter, 2002: NCEP-DEO AMIP-II Reanalysis (R-2). *Bul. Amer. Met. Soc.*, **83**, 1631–1643.
Koshlyakov, M.N., T.G. Sazhina, and A.Yu. Gol'din, 2001: Pacific-Antarctic cell of the global ocean conveyor. *Izvestiya, Atmospheric and Oceanic Physics*, **37**, 520–527.
Kozlov, V.F., and K.V. Koshel, 2000: A model of chaotic transport in the barotropic flow. *Izvestiya, Atmospheric and Oceanic Physics*, **36**, 119–128.
Resnyansky, Yu.D., and A.A. Zelenko, 1999: Effects of synoptic variations of atmospheric forcing in an ocean general circulation model: Direct and indirect manifestations. *Russian Meteorology and Hydrology*, **9**, 42–50.
Yang, H., 1996: Chaotic transport and mixing by ocean gyre circulation. *Stochastic Modeling in Physical Oceanography*, J. Adler, P. Muller, B. Rozovskii, Eds., Boston: Birkhauser, 434–466.
Zubov, N.N., 1938: Sea Waters and Ice. Hydrometizdat, Moscow, 453 pp. (in Russian).

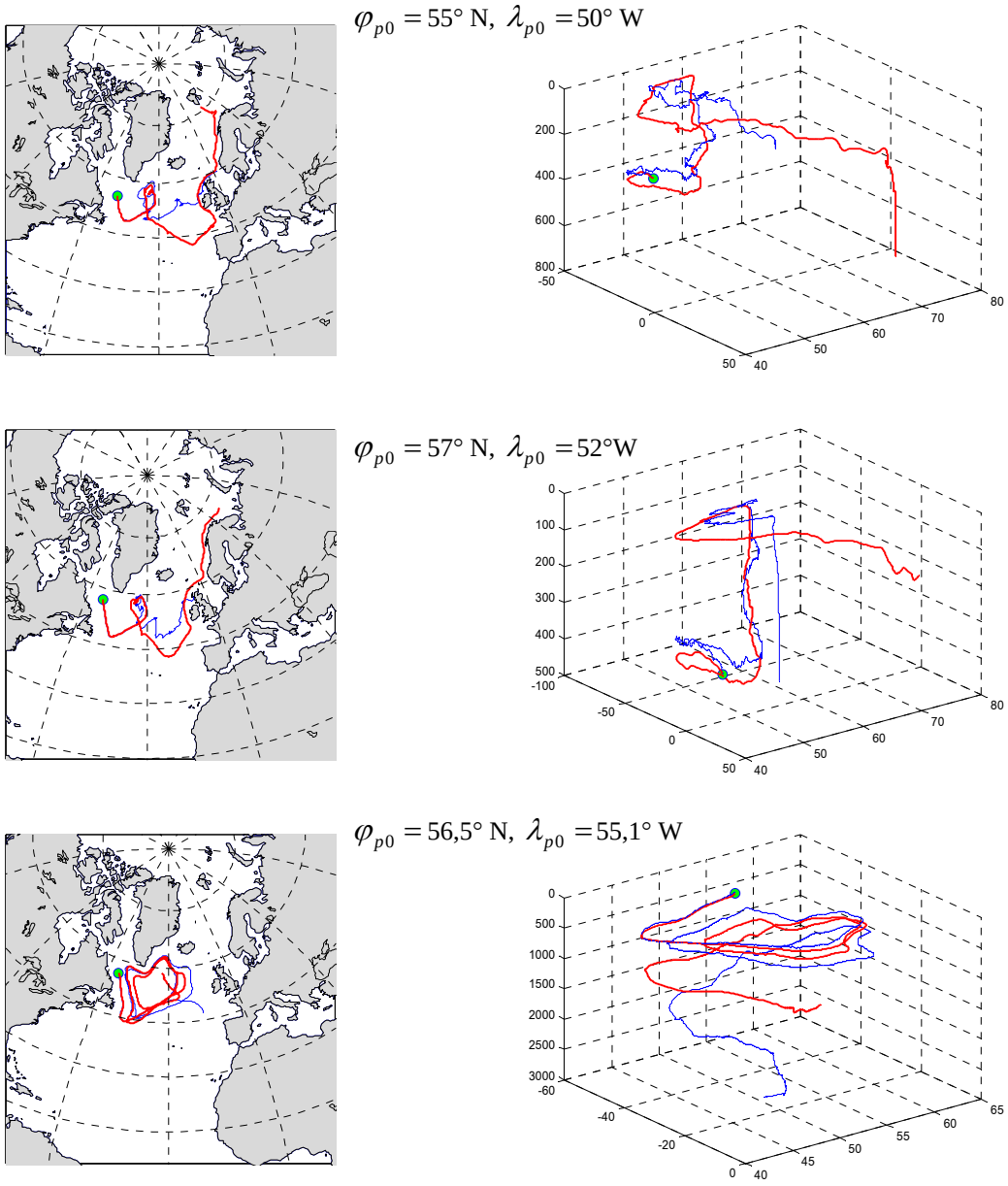

Fig. 1. Trajectories of liquid particles emitted from 500 m depth at three positions in the Labrador Sea. Left panels – horizontal projections of trajectories; right panels – their three-dimensional view. Computation using data on ocean currents from experiment ***BASE*** (6-hourly AF; blue thin lines) and from experiment ***SMON*** (monthly smoothed AF; red thick lines). The trajectories duration is 24 years (01.01.1979–31.12.2002). Green circles indicate initial position.

Near real-time temperature and salinity profiles in the Indian Ocean derived from TOPEX/POSEIDON altimetry

Bulusu Subrahmanyam[**], Wei Shi[#], and John M. Morrison[*]

[**]Marine Science Program & Department of Geology, University of South Carolina, Coulumbia, SC 29208, USA. (e-mail: sbulusu@geol.sc.edu)

[#]NOAA National Environmental Satellite, Data, and Information Service, University of Mayland Baltimore County, Camp Springs, MD 20746, USA. (e-mail: Wei.1.Shi@noaa.gov)

[*]Center for Marine Science, University of North Carolina Wilmington, Wilmington, NC 28409, USA. (e-mail: morrisonj@uncw.edu)

Abstract

The purpose of this paper is to show the potential of satellite altimetry in understanding the upper ocean temperature (T) and salinity (S) variability in the tropical Indian Ocean using a combination of TOPEX/Poseidon (T/P) derived sea-level anomalies, Reynold's sea surface temperature (SST), and monthly climatological T and S data (World Ocean Atlas, 1998). This new technique allows extension of altimetric surface information to derive the T and S information down to a depth of 1000 m. The accuracies of derived T and S profiles are evaluated using the World Ocean Circulation Experiment (WOCE) hydrographic data along Transindian Ocean Sections I1 and I3. This technique yields a difference of ~0.9°C or less between synthetic and observed (I1 section) temperature over most of the section, and a salinity difference of ~ 0.5 in the top 200 m and negligible difference beyond 200 m depth. The time series of synthetic T and S profiles constructed for the WOCE I1 and I3 sections shows the usefulness of this technique in obtaining information on the time variability of the water mass structure, currents, eddies, and propagating signals without having to carry out repeated hydrographic observations.

Methodology

We have adopted the technique developed by Shi et al. [2003] to derive the T, S profiles in the tropical Indian Ocean (30°N-30°S). Following this technique, quasi real-time T and S profiles were derived for the upper 1000 m water column for each 1° x 1° square during the period of 1993 –2000 using T/P sea surface height (SSH) anomalies, monthly climatological T and S profiles from the World Ocean Atlas 1998 (WOA 98).

Results

One of the advantages of this approach in estimating the T and S profiles is that it can be used to estimate the continuous temperature and salinity profiles in areas of sparse hydrographic data. The WOCE I1 section is the northernmost of the zonal sections carried out during the WOCE Indian Ocean Expedition during August 29-September 28, 1995 and September 30-October 16, 1995. It crossed the southern boundaries of both the Bay of Bengal (I1e) in the east (along 10°N latitude) and the Arabian Sea (I1w) in the west (along 8.5°N latitude), with 158 continuous profiles of temperature, salinity and oxygen versus pressure. Figure 1 displays a comparison between the observed temperature and salinity sections for WOCE I1 in the Arabian Sea and Bay of Bengal and the synthetic temperature and salinity sections derived using the method described above. A glance at the observed T and S WOCE I1 sections (Figure 1, top panel) and synthetic T and S sections (Figure 1 middle panel) shows that they are quite similar. In the Arabian Sea, on both temperature sections, the isotherms slope upward to the east below the mixed layer. In addition, the strong uplift of the isotherms along the western boundary

associated with the northeastward flowing Somali Current is clearly evident. The upper mixed layer is shallow in the eastern Arabian Sea and deepened in the western Arabian Sea along both sections. In both sections, SSTs in excess of 28°C are seen to the east of 62° E. Visual inspection shows that in the deeper layers, these two sections are also in close agreement. In both sections, the depression of the isotherms in the upper part of the water column associated with the "Great Whirl" is observed at ~57° E (although it is more obvious in the observed section). Within the Bay of Bengal, both sections show a mixed layer that is significantly shallower than the Arabian Sea. The thermocline deepens from west to east in the Bay of Bengal with the shallowest mixed layer found at ~85° E. In addition, both sections display a deepening of the isotherms along the east coast of Sri Lanka associated with the southwesterly flowing East Indian Coastal Current. Figure 1 (bottom panel) shows the errors of the T and S estimations. The largest errors in the T and S estimation are found at the depth of thermocline. Maximum temperature errors reach ~ 1.2°C, while the maximum error in salinity reaches ~ 0.5. Taking into account the limitations of the data used to construct the synthetic temperature and salinity fields, it appears that the technique used to construct these fields works quite well.

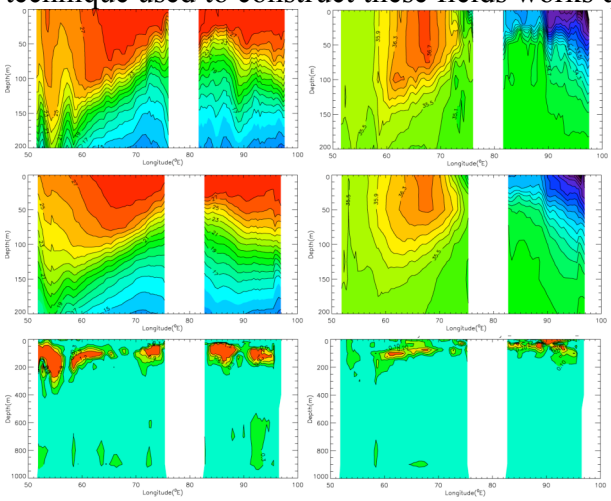

Figure 1. Comparison of (top panel) *in situ* temperature and salinity profiles along WOCE section I1, (middle panel) T/P derived temperature and salinity profiles, (bottom panel) the difference between *insitu* and T/P altimetry derived temperature and salinity profiles. Please note that top two panels are plotted to 200 m depth, whereas the bottom panel to 1000 m depth.

Conclusions

In this paper we have shown the methodology to separate out thermal (T) and salinity (S) signals from the satellite altimetric (T/P) SSH anomalies, and further applied this technique to the tropical Indian Ocean to derive near real-time T, S profiles in the upper 1000 m. This technique show that the generation of synthetic T and S profiles may be useful in studying the variability in the upper ocean, water mass structure and eddies without the need of repeat hydrographic section. This approach has only been tested in the Indian Ocean; further research is still required to see its applicability to other oceans.

Acknowledgements

The authors are extremely grateful to the TOPEX/Poseidon and JASON team at NASA/JPL and AVISO for provision of altimetry data. Bulusu Subrahmanyam was supported by NASA/JPL grant #961434 (TOPEX/Poseidon and JASON-1 altimetry).

References

Shi, W., B. Subrahmanyam , J.Morrison, Estimation of heat and Salt storage variability in the Indian Ocean from Topex/Poseidon altimetry, *J. Geophys. Res.*, 108 (C7), 3214, doi:10.1029/2001JC001244, 2003.

Development of New Techniques for Assimilating Satellite Altimetry Data into Ocean Models

Peng Yu, Steven L. Morey, and James J. O'Brien

Center for Ocean - Atmosphere Prediction Studies
Florida State University
Tallahassee, Fl 32306-2840
peng@coaps.fsu.edu

1. Introduction

State of the art fully three-dimensional ocean models are very computationally expensive, and the adjoint of them can be even more resource intensive, typically with ten times the computational cost or so. However, many features of interest can be approximated by the first baroclinic mode over much of the ocean, especially in the lower-mid latitude region. In order to fully take advantage of this characteristic and design a more efficient data assimilation system, a new type of data assimilation scheme, a reduced-space adjoint data assimilation technique, is developed, through the application of vertical normal mode decomposition (Philander 1990). To test this technique, the Navy Coastal Ocean Model (NCOM) (Martin 2000 and Morey et al. 2004) is used in the Gulf of Mexico as the forward model. The results indicate that the first baroclinic mode SSH represents the full SSH field very well. Twin experiments are run to test this method, and the dynamical field is recovered as expected and as fast as in around five iterations

2. Methods and Data

The assimilation procedure works by minimizing the cost function, which generalizes the misfit between the observations and their model counterparts (Ghil et. 1991), sea surface height (SSH) in this study, in a least-square sense. The model governing equations are integrated forward in time within the period during which the data are assimilated. Vertical normal mode decomposition is conducted to retrieve the first baroclinic mode, and the data misfit between the model outputs and observations is calculated. Adjoint equations based on a one active layer reduced gravity model, which approximates the first baroclinic mode, are integrated backward in time using the data misfit as the forcing to get the gradient of the cost function with respect to the control variables (velocity and SSH of the first baroclinic mode). The gradient is then input into an optimization algorithm, the limited memory BFGS method in this study, to determine the new first baroclinic mode velocity and SSH fields, which are used to update the NCOM model variables at the initial time.

SSH data from a forward NCOM run are sampled along Topex/POSEIDON (T/P) tracks to simulate the T/P observations. An EOF-based mapping method (Yu et. 2004) is then applied to produce a gridded dataset. The assimilated model fields are compared with the "truth" fields supplied by the twin experiment.

3. Results

The cost function reduces much faster after the first two iterations, and converges after five iterations (Figure 1).

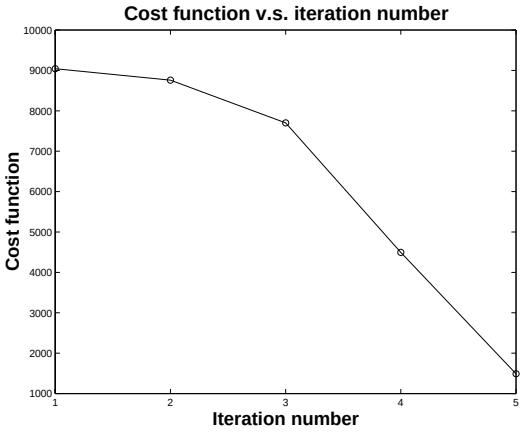

Fig. 1. Cost function v.s. iteration number for twin experiment.

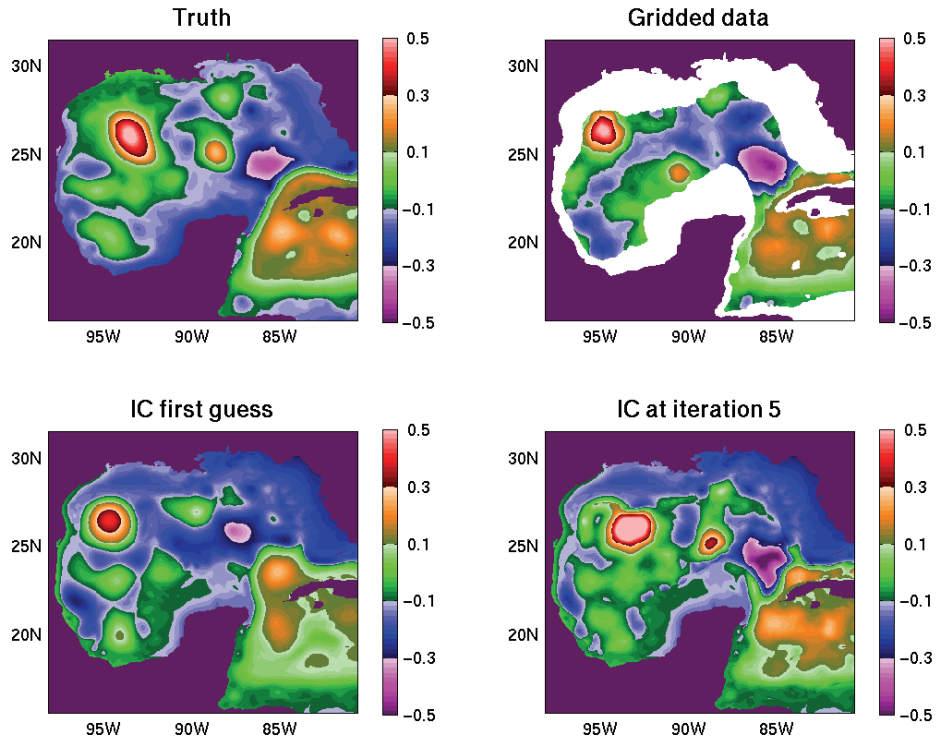

Fig 2. Sea surface height (SSH) field at model initial time. Upper left: The initial SSH field of "truth". Upper right: Gridded SSH data from the simulated Topex/POSEIDON data sampled from the truth field. Lower left: First guess of initial SSH field. Lower right: Initial SSH field after five iterations.

Figure 2 shows that after five iterations, the main features of the SSH field at initial time are very well recovered. Further studies show the comparison between other model variables and the "truth" fields is good, which indicates that this reduced-space adjoint technique is a powerful and efficient tool to improve the model initialization. Since the adjoint model has only one vertical layer compared to sixty vertical layers in the forward NCOM model, the computational cost is much lower.

Acknowledgements

This project was sponsored by the National Science Foundation, the Office of Naval Research Secretary of the Navy grant to James J. O'Brien, and by the NASA Office of Earth Science.

References

Ghil, M. and P. Malonotte-Rizzoli, Data assimilation in meteorology and Oceanograpy, *Adv. Geophys.*, *33*, 141-266, 1991.

Martin, P. J., 2000: The description of the Navy Coastal Ocean Model Version 1.0. NRL Report: NRL/FR/7322-009962, Naval Research Lab., Stennis Space Center, MS, 39pp.

Morey, S. L., P. J. Martin, J. J. O'Brien, A. A. Wallcraft, and J. Zavala-Hidalgo, Export pathways for river discharged fresh water in the northern Gulf of Mexico, *J. Geophys. Res.*, *108*, 3303-3317, 2003.

Philander, S. G., El Niño, La Niña, and the Southern Oscillation, pp. 160-167.

Yu, P., S. L. Morey, and J. Zavala-Hidalgo (2004), New mapping method to observe propagating features, *Sea Technology*, 45(5), 20-24.